isvr Institute of Sound and Vibration Research

Measurement of Bubbles in a Pipe Using Multiple Acoustic Techniques

T.G. Leighton, D.G. Ramble and A.D. Phelps

ISVR Technical Report No 258

June 1996

University of Southampton

SCIENTIFIC PUBLICATIONS BY THE ISVR

Technical Reports are published to promote timely dissemination of research results by ISVR personnel. This medium permits more detailed presentation than is usually acceptable for scientific journals. Responsibility for both the content and any opinions expressed rests entirely with the author(s).

Technical Memoranda are produced to enable the early or preliminary release of information by ISVR personnel where such release is deemed to the appropriate. Information contained in these memoranda may be incomplete, or form part of a continuing programme; this should be borne in mind when using or quoting from these documents.

Contract Reports are produced to record the results of scientific work carried out for sponsors, under contract. The ISVR treats these reports as confidential to sponsors and does not make them available for general circulation. Individual sponsors may, however, authorize subsequent release of the material.

UNIVERSITY OF SOUTHAMPTON

INSTITUTE OF SOUND AND VIBRATION RESEARCH

FLUID DYNAMICS AND ACOUSTICS GROUP

Measurement of bubbles in a pipe using multiple acoustic techniques

by

T. G. Leighton, D. G. Ramble and A. D. Phelps

ISVR Technical Report No. 258

June 1996

Approved: Group Chairman, P A Nelson
Professor of Acoustics

ACKNOWLEDGEMENTS

This work was funded by the Engineering and Physical Sciences Research Council ref: GR/H 79815.

CONTENTS

LIST OF FIGURES

and 'b'. The curved wall of the pipe (P) remote from the transducer can be seen in the lower half of frame 'b', and below it is an intense horizontal white region (A) indicating strong scattering from the pipe-air interface remote from the transducer.

ABSTRACT

This report describes the development of an acoustic system designed to detect, locate, and give the size distribution of gas bubbles in a pipe. This system uses both geometric and resonant procedures to locate and size / count the bubbles in the pipe, and the report describes the employment of several bubble resonance indicators and detection techniques which were implemented simultaneously. This allowed a greatly increased speed at which bubble populations could be measured, and ameliorated limitations inherent in individual techniques (such as give rise to errors when bubble populations are dense, or when turbulence or nonlinear distortion in the electronics are significant). Results are presented which were taken to study the potential of the location and sizing techniques on two test bubble populations, that of a single bubble tethered to a wire in the pipe, and for a freely rising bubble stream of one size.

I. INTRODUCTION

The ability to detect and size stable gas bubbles in a liquid is important to a range of applications [1,2]. The bubbles themselves may be significant in filling processes [3] (such as in the glass industry), material production (e.g. photographic industry), biomedical [4] and environmental applications [5, 6]. In addition, such stable bubbles may need to be characterised to asses the likelihood of inertial cavitation which they might seed in a liquid [7, 8], if it is to subsequently be subjected to high-amplitude pressure fluctuations (either acoustic or hydrodynamic). Many such applications would involve the detection of bubbles in pipes, ranging from the very large (e.g. in the petrochemical industry) to the very small (e.g. blood vessels).

Acoustic techniques are very suitable for bubble sizing, as there is a large impedance mismatch at the gas-liquid interface. The pulsation of a bubble approximates a lightly damped single degree of freedom system, where the mass component arises from the much denser liquid surrounding the bubble, the stiffness is attributable to the compressibility of the gas inside the bubble, and the damping is brought about through viscous losses at the wall, sound radiated into the fluid and thermal losses. As such it has a well defined resonance frequency, which for air bubbles in water at atmospheric pressure can be approximately expressed as:

$$\upsilon_0 R_0 \approx 3.2 \qquad Hz\,m \tag{1}$$

where υ_0 is the resonant frequency and R_0 is the equilibrium bubble radius. Thus from a knowledge of the acoustic resonance frequency of a bubble, its size can be readily determined.

It is possible to measure this resonance frequency by observing the strength of a backscattered acoustic signal, which is then assumed to be a maximum when the driving signal frequency (here termed the *pump* frequency ω_p) is coincident with a bubble resonance. However such estimates have poor spatial resolution, as at resonance the radii of bubbles are orders of magnitude smaller than the wavelength of the sound field, and provide ambiguous results, in that a bubble much larger than resonance may scatter more sound than a small resonant bubble [2]. This ambiguity may by reduced by monitoring the nonlinear behaviour of a bubble, as at large pulsation amplitude (typically taken to be an indicator of resonance) the bubble motion becomes increasingly asymmetric: as an obvious example, a bubble can theoretically expand without limit but only contract to zero radius. This results in the generation of integer related harmonics of the driving signal frequency at $2\omega_p$, $3\omega_p$ etc., and non-integer harmonics of the sound field, typically a subharmonic at $\omega_p/2$ and ultraharmonics at $3\omega_p/2$, $5\omega_p/2$ etc.

The long-term objective of this research was to provide an acoustic system which could analyse the population of gas bubbles in liquids in a pipe, in order first to determine the range of bubble radii present in the population (and the number of bubbles within each radius size class); and second to provide information on the spatial location of the bubbles within the liquid sample. It was originally proposed that this should be accomplished through exploitation of the nonlinear scattering properties of a bubble when it is insonated simultaneously with two acoustic fields: a high frequency fixed "imaging" beam (at angular frequency ω_i) and the lower frequency *pump* beam at angular

frequency ω_p tuned to the resonant frequencies of the bubbles under investigation. Though a range of combination frequency signals are generated when a bubble is insonated with two such frequencies, the objective was originally to analyse the bubble population using the signal scattered at $\omega_i \pm \omega_p/2$, since it had previously been shown that of all the resonant bubble signals, this one gave the only unambiguous indicator of a resonant bubble, and also the best radius resolution [1, 2, 9]. This is because the signal is stimulated only when the pump frequency is very close to the bubble resonance (within about 10 Hz), and, as the signal is parametric in nature, only when the amplitude of the pump field is above a known threshold pressure. This means that if an unknown bubble population is insonated by an imaging field at fixed frequency ω_i, and by a pump field whose frequency (ω_p) is incremented, the scattering at $\omega_i \pm \omega_p/2$ can be most readily related back to the resonant bubbles in the population [9].

The two objectives of the research were achieved through a combination of resonant and geometrical scattering techniques. The problem of spatial resolution was addressed through the use of a 3.5 MHz ultrasonic scanner, whose operational frequency is much higher than any potential bubble resonance, and the bubble sizes were then investigated through the use of an unfocused imaging beam. Dividing the measurement between resonant and geometric techniques allowed the speed of measurement (of, for example, a pipe cross-section) to be increased substantially.

The success of the combination of these two techniques inspired further investigations along these lines. Further increases in the speed of measurement were achieved by reducing the prospective range of frequencies within which any bubble resonances might lie, and through which the pump frequency had to be incremented at a rate of one increment (of, say, 25 Hz) per 1.6 s. As this requires prior knowledge of the range of bubble sizes present, a broadband insonation was employed: In 0.2 s enough data could be collected to reduce the range through which the pump frequency must be incremented from 7 kHz to 1 kHz, further decreasing the measurement time by almost another order of magnitude [10].

With improved knowledge of the mechanism of generation of the $\omega_i \pm \omega_p/2$ signal [9, 11] came the ability to manage a compromise between speed of measurement and uncertainty in the measured radii [10] in a predictable fashion. However what remained were the fundamental limitations imposed by the physics of the $\omega_i \pm \omega_p/2$ signal [11]. Different limitations arise when bubbles are sized using any acoustic signal (such as scatter of the harmonics (ω_p, $2\omega_p$, $3\omega_p$...), subharmonic ($\omega_p/2$) and ultraharmonics of the bubble resonance). However, it was realised that with the existing equipment one was not limited to use of the signal at $\omega_i \pm \omega_p/2$ alone: when a bubble is insonated at both pump and imaging frequencies, a wide spectrum of signals may be generated (ω_p, $2\omega_p$, $3\omega_p$; $\omega_p/2$, $3\omega_p/2$;, $\omega_i \pm \omega_p$, $\omega_i \pm \omega_p/2$, $\omega_i \pm 2\omega_p$ etc.) and the simultaneous analysis of all these signals can be optimised to best obtain the measurement of the bubble radii present [10].

In this way the principle of COBUST ("Characterisation of Bubbles Using Simultaneous Techniques") was realised [12], where by the simultaneous use of several techniques allows the limitations of any one to find compensation through the use of the others. Following the significant success of the technique in tank tests [10, 13, 14], COBUST was deployed in a pipe to size and localise bubbles. In principle not only should the use of COBUST, as opposed to the technique originally envisaged, achieve this objective at a

greatly increased measurement speed, but also with the minimisation of any ambiguity. This report examines the sensitivity limits of the apparatus for bubble detection and sizing, and discusses the requirements for an 'ideal' bubble detector.

II. METHOD

II a - The COBUST Principle

The principle by which COBUST operates is that individual techniques for bubble sizing have their limitations which are overcome by simultaneous deployment. For example, if a liquid containing bubbles is insonated with a pump frequency ω_p, then strong scattering at ω_p may be the result of resonant bubbles, or may be the result of geometrical scattering from large bubbles [1]: used on its own, there is no way to distinguish between these two. However the generic COBUST apparatus, shown schematically in figure 1, overcomes this problem by comparing different signals [14]. Upon injection from a nozzle the bubble may be sized from its passive acoustic emissions (an exponentially-decaying sinusoid shown in Figure 1a). The pump signal is generated at ω_p (by the Pump signal transducer) and the scattered spectrum analysed in terms of the harmonics, subharmonic and ultraharmonics (as shown in Figure 1c). By additionally introducing the high frequency "imaging" transmitter and receiver, the spectrum of combination frequencies can also be analysed, and the bubble presence inferred through the scattering of signals at $\omega_i \pm \omega_p$, $\omega_i \pm 2\omega_p$, $\omega_i \pm \omega_p/2$, etc. (Figure 1d). In addition geometrical scattering using a 3.5 MHz scanning system is shown in Figure 1b. Though the wavelength is in general not sufficiently small to obtain good radius resolution directly, certain information can be inferred from the rise time as measured in the M-mode of the scanner operation [10].

II b - The Pipe Tests

The specific experimental arrangement used for the pipe tests is shown photographed in figures 2a and b, and diagrammatically in figure 3. The bubbles can be injected at the base of the pipe, which has internal diameter of 10 cm, their passive emissions being detected by the lower hydrophone (HP2) and used for sizing [10]. They rise through the beam of the 3.5 MHz ultrasonic scanner (Hitachi EUB-26E), and are then driven by the pump signal, which is generated by the ring transducer. The upper hydrophone (HP1) can be incorporated into the pipe wall or, as shown in Fig. 3, immersed in the liquid. It detects the scattering of the harmonics and subharmonics of the fundamental resonance. The beam patterns of the imaging frequency projector and receiver overlap within the region of the pipe surrounded by the ring transducer.

As an initial test, the signals detected when a single bubble is tethered in this region are shown in figure 4. The direct scattered signal at ω_p is presented in Fig. 4a; $2\omega_p$ in Fig. 4b; and $\omega_p/2$ in Fig. 4c. The heterodyned signals at $\omega_i \pm \omega_p$, $\omega_i \pm 2\omega_p$ and $\omega_i \pm \omega_p/2$ are shown in figures 4d to 4f respectively. All are taken simultaneously as the pump signal is incremented in 50 Hz steps from 4 to 5 kHz, at an amplitude of 120 Pa. The bubble-mediated amplification (i.e. the ratio of the 'bubble present' to 'bubble absent' signal levels) is plotted for the scattering at ω_p, $2\omega_p$ and $\omega_p/2$, but because the MHz noise floor is so low (shown as broken lines in Figs. 4d to 4f), the signal strength relative to the

average noise floor is plotted for the $\omega_i \pm \omega_p$, $\omega_i \pm 2\omega_p$ and $\omega_i \pm \omega_p/2$ signals. The bubble resonance is best indicated by the $\omega_i \pm \omega_p/2$ signal to be 4500 ± 50 Hz; the $\omega_i \pm \omega_p$ signal peaks in this region but its frequency spread is much larger. In contrast, the $\omega_i \pm 2\omega_p$ signal, although it also peaks around 4500 Hz, does not rise sufficiently out of the noise to provide an unambiguous bubble indicator. The scatter of the fundamental, ω_p, shows the expected through-resonance behaviour, centred around 4500 ± 100 Hz, but neither the second harmonic nor subharmonic signals reliably indicate the presence of a single bubble. From these resonance frequency estimates, the radius of the bubble can be estimated as 740 ± 8 μm.

Clearly any one signal alone would have provided a less clear picture of the bubble population. This fact becomes far more obvious when the more realistic system, that of rising bubbles, is studied, where a varied population and the inclusion of Doppler and turbulence effects can complicate the signals. Data taken when sizing a stream of rising bubbles is presented in figures 5 and 7, with the direct scattered signals at ω_p, $2\omega_p$ and $\omega_p/2$ shown in figures 5a to c respectively, and the heterodyned combination frequency results (taken simultaneously) shown in figure 6. Here, the bubble stream was insonated with the pump transducer between 3.5 and 4.5 kHz in 50 Hz steps, and at an amplitude of 150 Pa. From the direct scattered signals, only the result at ω_p (shown in figure 5a) gives any indication of the bubbles' resonance, at 4000 ± 200 Hz. In contrast the greyscale plot of the power spectrum of the heterodyned combination-frequency scattered signal (Figure 6) shows a clear peak in the $\omega_i \pm \omega_p/2$ signal at 3950 ± 50 Hz, with a similar but less pronounced peak evident in the $\omega_i \pm \omega_p$ signal. At each signal location, the $\omega_i + \omega_p/2$ and $\omega_i - \omega_p/2$ signals are separately resolvable, as a result of the Doppler shift before heterodyning. A similar effect is seen in the $\omega_i \pm \omega_p$ signals, allowing an estimate of the bubbles' radii of 840 ± 11 μm.

Motion information is most clearly determined through the simultaneous M-mode operation of the 3.5 MHz ultrasound scanner, shown in figure 7a, where the horizontal axis represents the time scale (of duration 2s) for objects moving through the line shown in the centre of the B-mode image (figure 7b). Bubbles therefore show as almost vertical streaks in M-mode, their gradient giving the rise time (from which an estimate of the bubble size can be made [10]). In b) the bubbles can be seen crossing the white line in the centre of the frame. This frame represents a horizontal cross-section of the pipe, the 18 cm distance in the field from the transducer face (which is at the top of the frame) being indicated by centimetre-spaced markings on the border between frames 'a' and 'b'. The curved wall of the pipe remote from the transducer can be seen in the lower half of frame 'b', and below it is an intense horizontal white region indicating strong scattering from the pipe-air interface remote from the transducer.

III. DISCUSSION

The deployment of COBUST in a pipe can be compared against an *Ideal objective* [12, 13] which can be formulated for a bubble sizing system. The system would deploy a range of these techniques to interrogate a given liquid sample, either sequentially or concurrently as defined by the problem. This would enable optimisation of the process of characterising the bubble population in the liquid with respect to minimising the

ambiguity of the result and the complexity of the task. The task itself involves first the detection of inhomogeneities in liquids. In certain circumstances it is then necessary to analyse the sample further to distinguish gas bubbles from solid or immiscible liquid-phase inclusions. The final stage of analysis would involve not only the detection, but also the sizing of the gas inclusions, leading to the characterisation of the bubble population. The *Ideal Objective* therefore be summarised through the following goals:

(i) Detect inhomogeneities in liquids
(ii) Distinguish gas bubbles from solids
(iii) Measure radii of gas inclusions present
(iv) Measure number of bubbles in each radius class.

The pipe system discussed in this paper contains the necessary basis for satisfying this objective. As bubbles pass through the field of the Hitachi scanner, M-Mode operation indicates the presence of a moving body having a specific acoustic impedance significantly different to that of the liquid. Its position is recorded on the B-mode image, which will also roughly indicate the number of inhomogeneities, or whether there is a massive obstruction (such as an air plug). However geometrical scattering on its own cannot distinguish between solid and gaseous inhomogeneities, nor give an accurate measure of size. However the inhomogeneity then passes through the ring transducer, which can make the distinction: resonant scattering of the pump signal by a bubble is many orders of magnitude stronger than that from a solid body of similar size [15]. In this test therefore of the current system satisfies the first three components of the *Ideal Objective*: since the objective was to examine the sensitivity limits, the fourth is not applicable. To satisfy that, the ability of the individual techniques to give such measures must be relied upon, and these can be found in the literature [15-27]. With increasingly dense populations errors may occur: however there is no reason in principle why other sizing systems, such as the inclusion of a resonator [28, 29], may not be incorporated against such an eventuality.

For the detection of the passage of transient inhomogeneities, broadband insonation must be used, since with the current data acquisition system it has been possible to cover a 7 kHz range with 90 Hz resolution in only 0.2 s [10], a speed unattainable with incremented tone techniques. The greater radius resolution which an incremented pump frequency provides can be exploited to examine steady-state populations. Automation of such a system, so that the triggering of the ultrasonic scanner by the passage body causes activation of the pump and imaging transducers, is feasible. Passive acoustic emissions are sensitive to air entrainment, and so may be used in leak detection (though background noise within the same frequency band may necessitate the employment of suitable signal processing [30]).

IV. CONCLUSION

A liquid-filled pipe has been instrumented to determine the radii of bubbles present within the pipe. The use of simultaneous systems, as opposed to a lone system, decreases the likelihood of error. The current system is capable of detecting and sizing as few as a single bubble present in the detection volume.

V. REFERENCES

1 **Leighton, T.G.** 'Acoustic Bubble Detection I. - the detection of stable gas bodies', *J Soc Env Eng*, **7**, 9-16 (1994)

2 **Leighton, T.G.** *The Acoustic Bubble* (Academic Press, London, 1994)

3 **Detsch, R.M. & Sharma, R.N.** 'The critical angle for gas bubble entrainment by plunging liquid jets', *The Chemical Engineering Journal,* 157-166 (1990)

4 **Tickner, E.G.** 'Precision microbubbles for right side intercardiac pressure and flow measurements', In: *Contrast Echocardiography* edited by Meltzer, R.S. and Roeland, J. (Nijhoff, London, 1982)

5 **Woolf, D.K.** 'Bubbles and the air-sea transfer velocity of gases', *Atmos-Ocean,* **31**, 451-474 (1993)

6 **Thorpe, S.A.** 'Measurements with an Automatically Recording Inverted Echo Sounder; ARIES and the Bubble Clouds', *J Physical Oceanography,* **16,** 1462-1478 (1986)

7 **Leighton, T.G.** 'Acoustic Bubble Detection II - the detection of transient cavitation.', *J Soc Env Eng*, **8**, 16-25 (1995)

8 **Leighton, T.G.** 'Bubble population phenomena in acoustic cavitation', *Ultrasonics Sonochemistry*, **2**, S 123-136 (1995)

9 **Phelps, A.D. & Leighton, T.G.** 'High resolution bubble sizing through detection of the subharmonic response with a two frequency excitation technique', *J Acoust Soc Am,* **99**, 1985-1992 (1996)

10 **Leighton, T.G, Ramble, D.G. & Phelps, A.D.** 'Comparison of the abilities of multiple acoustic techniques for bubble detection', *Proc Inst of Acoustics,* **17** (8), 149-160 (1995)

11 **Phelps, A.D. & Leighton, T.G.** 'The subharmonic oscillations and combination frequency emissions from a resonant bubble', *Acta Acustica,* (In press, 1996)

12 **Leighton, T.G., Phelps, A.D., Ramble, D.G. & Sharpe, D.A.** 'Comparison of the abilities of eight acoustic techniques to detect and size a single bubble', *Ultrasonics,* (In press, 1996)

13 **Ramble, D.G. & Leighton, T.G.** 'The use of multiple acoustic techniques to size tethered and rising bubbles', *ISVR Technical Report No. 250, University of Southampton* (1995)

14 **Leighton, T.G., Phelps, A.D. & Ramble, D.G.** 'Acoustic bubble sizing: from laboratory to the surf zone trials', *Acoustics Bulletin,* (In press, 1996)

15 **Medwin, H.** 'In situ acoustic measurements of microbubbles at sea', *J Geophys Res*, **82,** 971-976 (1977)

16 **Farmer, D.M. & Vagle, S.** 'Waveguide propagation of ambient sound in the ocean-surface bubble layer', *J Acoust Soc Am,* **86,** 1897-1908 (1989)

17 **Nishi, R.Y.** 'Ultrasonic detection of bubbles with Doppler flow transducers', *Ultrasonics,* **10,** 173-179 (1972)

18 **Blackledge, J.M.** 'B-scan imaging of two phase flows', *IEE Colloquium on Ultrasound in the process industry, September 23rd,* 5/1-5/17 (1993)

19 **Morriss, S.L. & Hill, A.D.** 'Ultrasonic imaging and velocimetry in two-phase pipe flow', *Trans ASME,* **115,** 108-116 (1993)

20 **Van der Welle, R.** 'Void fraction, bubble velocity and bubble size in two phase flow, *Int J Multiphase Flow,* **11**(3), 317-45 (1985)

21 **Kolbe, W.F., Turko, B.T. & Leskovar, B.** 'Fast ultrasonic imaging in a liquid filled pipe', *IEEE Trans Nucl Sci,* **33**(1), 715-722 (1986)

22 **Miller, D.L.** 'Ultrasonic detection of resonant cavitation bubbles in a flow tube by their second harmonic emissions', *Ultrasonics,* **19**, 217-224 (1981)

23 **Miller, D.L., Williams, A.R. & Gross, D.R.** 'Characterisation of cavitation in a flow-through exposure chamber by means of a resonant bubble detector', *Ultrasonics,* **22,** 224-230 (1984)

24 **Schmitt, R.M., Schmitt, H.J. & Siegert, J.** '*In vitro* estimation of bubble diameter distribution with ultrasound', *IEEE Eng in Med and Biol Soc, 9th Annual Conference,* 13-6 (1987)

25 **Newhouse, V. L. & Shankar, P. M.** 'Bubble size measurement using the nonlinear mixing of two frequencies', *J Acoust Soc Am,* **75,** 1473-1477 (1984)

26 **Koller, D., Li, Y., Shankar, P.M. & Newhouse, V.L.** 'High-speed bubble sizing using the double frequency technique for oceanographic applications', *IEEE J Oceanic Engineering,* **17,** 288-291 (1992)

27 **Phelps, A.D. & Leighton, T.G.** 'Investigations into the use of two frequency excitation to accurately determine bubble sizes', *Bubble Dynamics and Interface Phenomena. Proceedings of an IUTAM symposium held in Birmingham, UK, 6-9 September 1993* edited by J. R. Blake *et al* (Kluwer Academic Press, Netherlands, 1994), 475-483

28 **Breitz, N. & Medwin, H.** 'Instrumentation for in situ acoustical measurements of bubble spectra under breaking waves', *J Acoust Soc Am,* **86**, 739-743 (1989)

29 **Medwin, H. & Breitz, N.D.** 'Ambient and transient bubble spectral densities in quiescent seas and under spilling breakers', *J Geophys Res,* **94,** 12751-12759 (1989)

30 **Leighton, T.G., Schneider, M.F. & White, P.R.** 'Study of bubble fragmentation using optical and acoustic techniques', *Sea Surface Sound '94* edited by M.J. Buckingham and J.R. Potter, (World Scientific Publishing Ltd., Singapore, 1995) 414-428

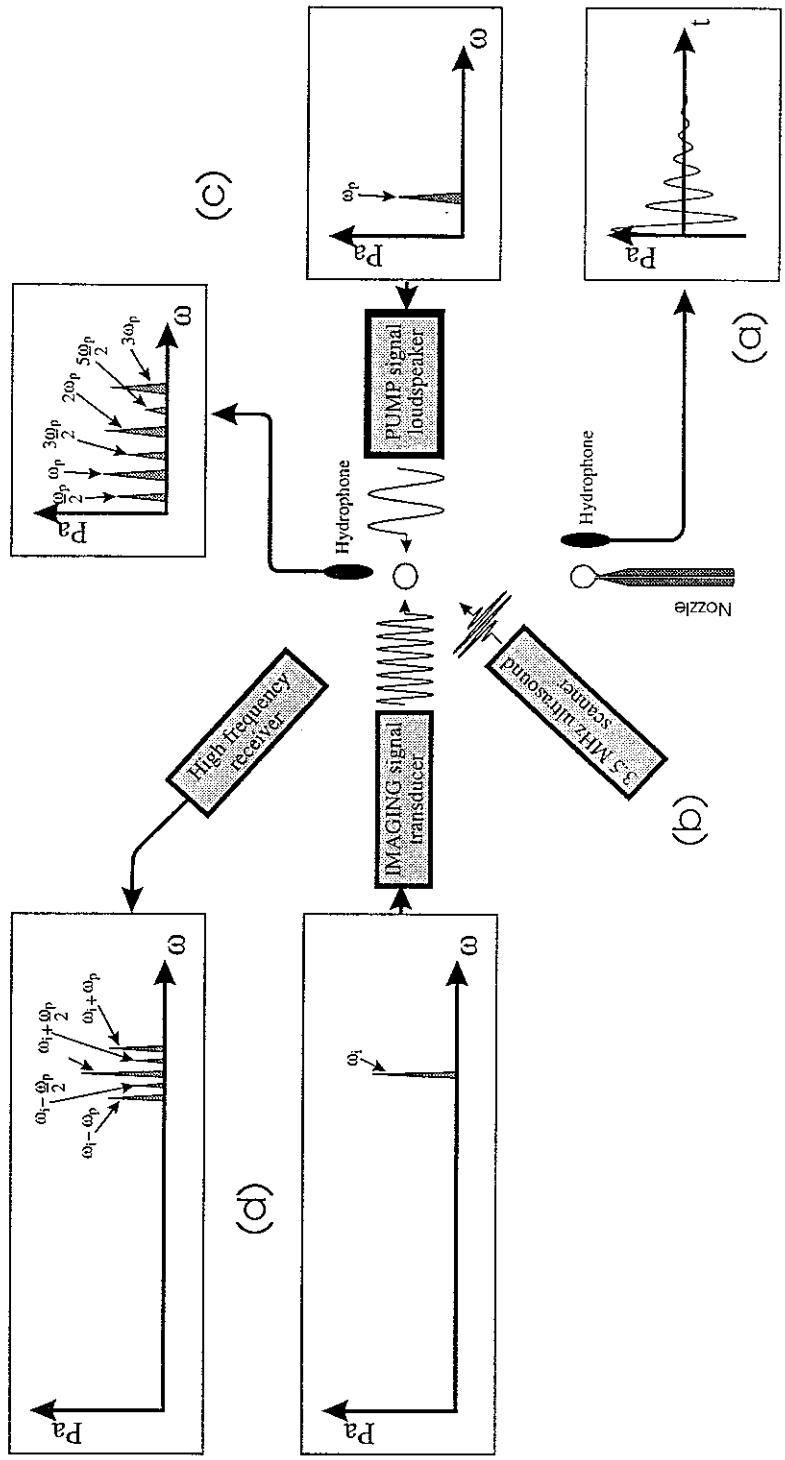

Figure 1 - Schematic of the apparatus required to implement the various acoustic detection techniques. In (a) the bubble is shown, injected from a nozzle, where a hydrophone detects its short duration passive emissions. In contrast, all the active techniques are schematically shown interrogating a bubble which has risen under buoyancy. In (b) a medical diagnostic ultrasound scanner is deployed to produce an image of the bubble (shown in Figure 2). In (c) the pump transducer generates a series of tonal pump signals, and a second hydrophone detects structure in the spectrum corresponding to $2\omega_p$, $3\omega_p$, $\omega_p/2$, $3\omega_p/2$ and $5\omega_p/2$ in the presence of a resonant bubble. In (d) a high frequency imaging signal is projected onto the bubble, and the scattered signal is detected by a high frequency receiver. Whilst in the absence of the bubble, ideally only ω_p and ω_i can be should be present, a resonant bubble will produce structure in the spectrum around ω_i.

a)

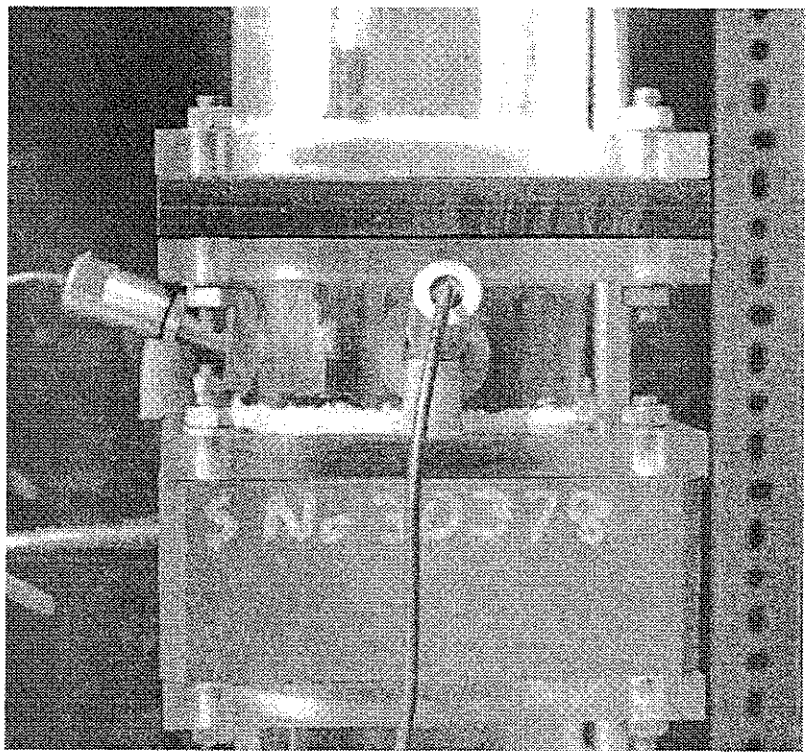

b)

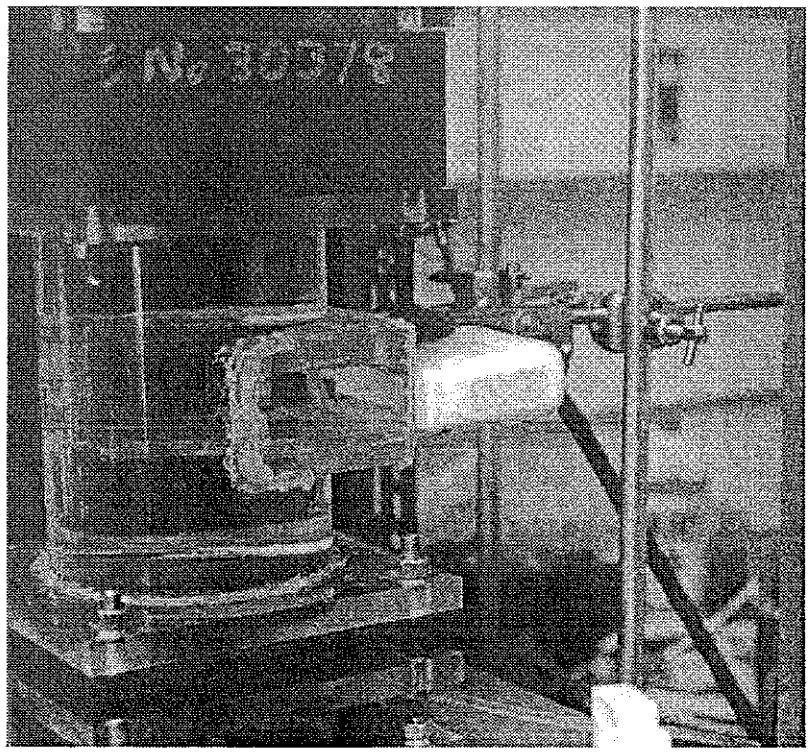

Figure 2 - Photograph of the apparatus used in the measurements of bubbles in a pipe, a) high frequency transducers and the ring pump transducer, and b) 3.5 MHz scanning equipment.

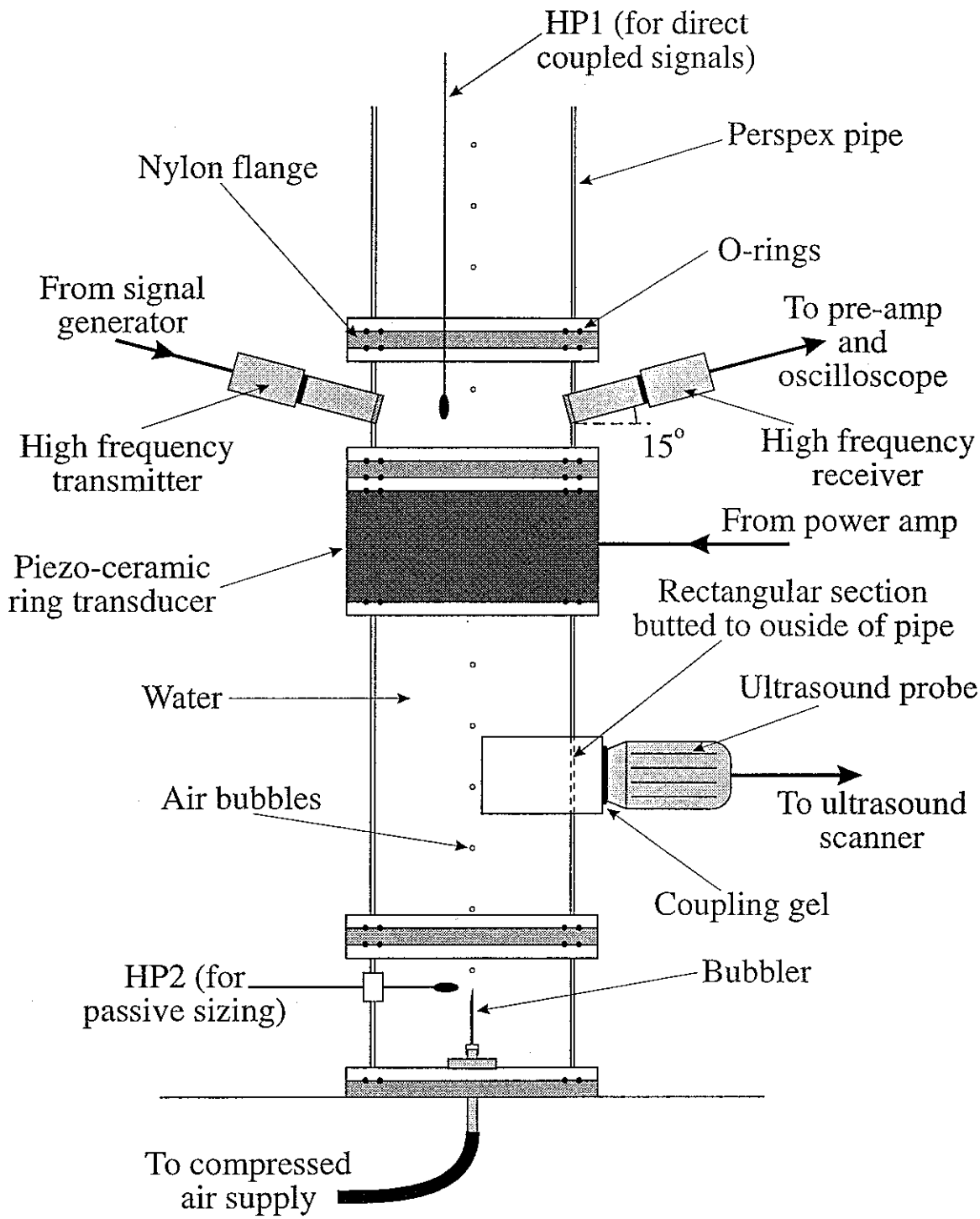

Figure 3 - Schematic of the apparatus used in the measurements of bubbles in a pipe.

Fig 4

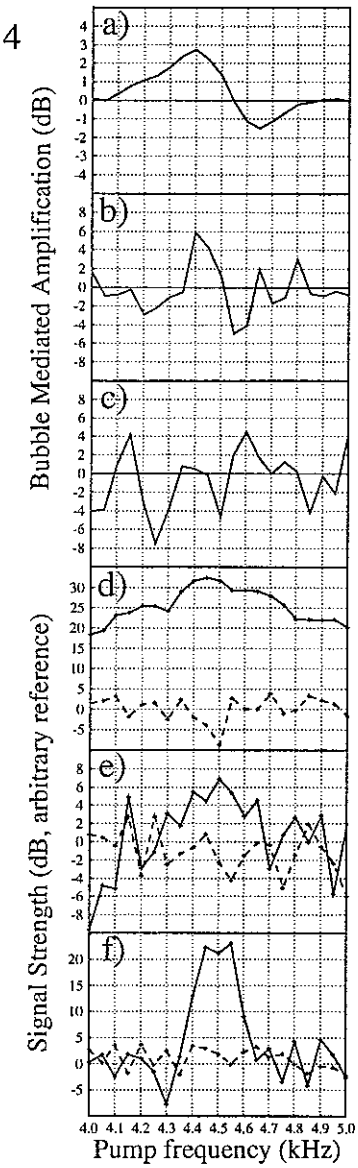

Fig 5

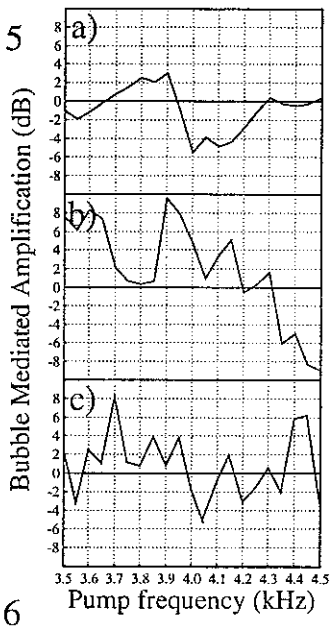

Fig 6

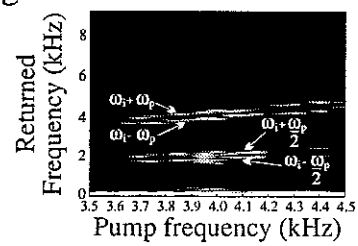

Fig 7

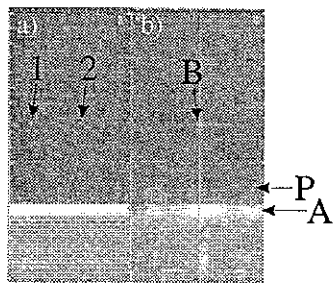

Figure 4 - Results from measurements of a stationary bubble tethered to a wire in the transducer focus in the pipe. The bubble was insonated between 4 kHz and 5 kHz in 50 Hz steps through its resonance at an amplitude of 120 Pa. Signals shown are at: a) ω_p, b) $2\omega_p$, c) $\omega_p/2$, d) $\omega_i \pm \omega_p$, e) $\omega_i \pm 2\omega_p$ and f) $\omega_i \pm \omega_p/2$.

Figure 5 - Low frequency backscattered results from measurements at a) ω_p, b) $2\omega_p$, and c) $\omega_p/2$, on rising bubbles. The bubbles were insonated between 3.5 and 4.5 kHz in 50 Hz steps at an amplitude of 150 Pa.

Figure 6 - High frequency backscattered results taken simultaneously to the results shown in figure 4. The grey-scale plot shows areas of high signal strength in white. The frequency spectra of the 'Returned' signal (which has been heterodyned), obtained for each setting of the pump frequency (shown on the horizontal axis), have been plotted side-by-side to form a single grey-scale representation, emphasising the changes in the spectral components. The sum-and-difference peaks are separated due to a Doppler shift on the returned signal.

Figure 7 - Results from the 3.5 MHz ultrasonic scanner. a) M-mode scan, recording (against time over a 2s period plotted on the horizontal axis) the position of images which cross the vertical white line in the centre of b) the B-mode image. Bubbles (1&2) therefore show as almost vertical streaks, their gradient giving the rise time. In b) the bubbles (B) can be seen crossing the white line in the centre of the frame. This frame represents a horizontal cross-section of the pipe, the 18 cm distance in the field from the transducer face (which is at the top of the frame) being indicated by centimetre-spaced markings on the border between frames 'a' and 'b'. The curved wall of the pipe (P) remote from the transducer can be seen in the lower half of frame 'b', and below it is an intense horizontal white region (A) indicating strong scattering from the pipe-air interface remote from the transducer.